JOURNAL OF MATERIALS SCIENCE 31 (1996) 699–705

Perovskite phase formation and microstructural evolution of lead magnesium tungstate–lead titanate ceramics

CHUNG-HSIN LU
Department of Chemical Engineering, National Taiwan University, Taipei, Taiwan, Republic of China

The perovskite phase formation and microstructural evolution in the $Pb(Mg_{0.5}W_{0.5})O_3$–$PbTiO_3$ system have been investigated in this work. During the solid-state reaction of $Pb(Mg_{0.5}W_{0.5})O_3$, only $PbWO_4$ and Pb_2WO_5 are formed as intermediate phases at low temperature range. Moreover, the perovskite phase $Pb(Mg_{0.5}W_{0.5})O_3$ begins to form at 600 °C and is complete at 850 °C. As $Pb(Mg_{0.5}W_{0.5})O_3$ is doped with $PbTiO_3$, the formation of the perovskite phase becomes sluggish and the temperature for the complete reaction to take place increases up to 1000 °C. The doping of the $Pb(Mg_{0.5}W_{0.5})O_3$ with $PbTiO_3$ apparently induces the formation of a small amount of liquid phase, which is possibly attributed to a reaction with residual Pb_2WO_5. This liquid phase not only accelerates the densification of specimens through a liquid phase sintering mechanism, but also causes abnormal grain growth, thereby forming an inhomogeneous microstructure. The dielectric permittivity of $Pb(Mg_{0.5}W_{0.5})O_3$ does not depend on frequency, and a sharp phase transformation from the antiferroelectric to the paraelectric state occurs at around 40 °C. In contrast, the dielectric properties and broad phase transformation temperatures of $Pb(Mg_{0.5}W_{0.5})_{0.9}Ti_{0.1}O_3$ and $Pb(Mg_{0.5}W_{0.5})_{0.6}Ti_{0.4}O_3$ strongly depend on frequency. This dependency would imply that the $PbTiO_3$ addition to $Pb(Mg_{0.5}W_{0.5})O_3$ alters the order arrangement of B-site cations to a disordered state and induces relaxor-ferroelectric characteristics.

1. Introduction

Multilayer ceramic capacitors (MLCCs) have become the dominant variety of capacitors used in the electronics industry because of their compact dimension and high electronic quality. A tremendous amount of research has been devoted towards new dielectric materials and new fabrication technologies to increase the capacitance, quality, and reliability of MLCCs. Besides improving these electronic properties, intensive efforts have recently been aimed towards reducing the cost of MLCCs for the sake of increasing competitiveness and profitability. The fundamental concept behind cost reduction involves substituting the noble metal used in the inner electrodes with the less expensive silver/palladium alloys [1] or other base metals, e.g. nickel [2]. Silver/palladium is stable at elevated temperatures; however, in contrast, nickel suffers from severe oxidation when heated in an air atmosphere. Although the thermal stability of silver/palladium is superior to that of nickel, the melting temperature of the former material is lower than the sintering temperature of conventional $BaTiO_3$-based ceramics. Therefore, in order to allow the ceramics to fit the melting characteristic of silver/palladium, developing new dielectric ceramics which can be sintered at low temperatures is considered to be one of the most practical approaches.

Lead magnesium tungstate ($Pb(Mg_{0.5}W_{0.5})O_3$)-based ceramics have been known as dielectric materials possessing low dissipation loss and low sintering temperatures (lower than 1000 °C) [3]. These ceramics are one of the potential materials to be utilized in multilayer capacitors, and they can be co-fired with silver/palladium inner electrodes. $Pb(Mg_{0.5}W_{0.5})O_3$ was first synthesized by Smolenskii *et al.* [4] in 1959, and was found to exhibit a perovskite crystalline structure possessing antiferroelectric properties at room temperature. Crystallographic and dielectric properties of $Pb(Mg_{0.5}W_{0.5})O_3$-based solid solutions have been widely investigated [5–10]. Bouchard *et al.* [11] first used $Pb(Mg_{0.5}W_{0.5})O_3$ and lead titanate ($PbTiO_3$) to fabricate low-temperature firing materials for multilayer capacitors. Later Yonezawa and other researchers [12, 13] added the third component $Pb(Ni_{0.33}Nb_{0.67})O_3$ to modify the dielectric properties of the above binary system. The dielectric constant and specific resistivity were increased by adding an appropriate amount of $Pb(Ni_{0.33}Nb_{0.67})O_3$; nevertheless, the addition of $Pb(Ni_{0.33}Nb_{0.67})O_3$ increased the sintering temperatures of the specimens. DTA analysis in the $Pb(Ni_{0.33}Nb_{0.67})_x(Mg_{0.5}W_{0.5})_{0.5-0.5x}Ti_{0.5-0.5x}O_3$ ($x = 0$–0.4) system revealed the formation of a liquid phase at around 880 °C in all specimens [12]. Notably, the liquid phase was present no matter whether

0022–2461

$Pb(Ni_{0.33}Nb_{0.67})O_3$ was added or not. Therefore, this would imply that the liquid phase is formed in the $Pb(Mg_{0.5}W_{0.5})O_3$–$PbTiO_3$ system. However, the presence of this liquid phase has not yet been confirmed. Furthermore, its influence on the microstructure remains unclear.

The aim of this work was first to elucidate the reaction process in the $Pb(Mg_{0.5}W_{0.5})O_3$–$PbTiO_3$ system. Additionally, the formation sequence of perovskite phase was deduced. This work also investigated the formation of a liquid phase in $PbTiO_3$-doped $Pb(Mg_{0.5}W_{0.5})O_3$ as well as the effects of the liquid phase on the evolution of microstructural features. Furthermore, the dielectric characteristics and phase-transition behaviour of $Pb(Mg_{0.5}W_{0.5})O_3$–$PbTiO_3$ ceramics were analysed.

2. Experimental details

2.1. Specimen preparation

According to the composition $Pb(Mg_{0.5}W_{0.5})O_3$, $Pb(Mg_{0.5}W_{0.5})_{0.9}Ti_{0.1}O_3$ (10 mol % $PbTiO_3$ addition), and $Pb(Mg_{0.5}W_{0.5})_{0.6}Ti_{0.4}O_3$ (40 mol % $PbTiO_3$ addition), three kinds of raw materials were prepared using appropriate amounts of PbO, MgO, WO_3, and TiO_2. Each batch was ball-milled for 48 h with ethyl alcohol, using resin-coated iron balls in a resin mill. After drying in a rotary evaporator under reduced pressure, the powder was ground and filtered through a 100-mesh screen to eliminate agglomerated powder. The dried powder was uniaxially pressed into discs of 8 or 10 mm in diameter under 98 MPa. The prepared dried powder and pressed discs were used for the following experiments.

2.2. Characterization

Differential thermal analysis (DTA) was conducted to examine the variation of heat during the reaction for each specimen. In order to investigate solidification behaviour of the liquid phase, subsequent cooling was carried out after a heating run for given temperatures. The heating and cooling rates were 5 °C min^{-1}, and Al_2O_3 was used as the standard material. Each specimen was heated to the desired temperatures and quenched in air. The compounds present in the specimens were identified by performing X-ray powder diffraction (XRD) analysis using CuK_α radiation. The formation fraction of each compound was semi-quantitatively calculated by the following equation

$$\text{relative intensity of i (\%)} = I_i/\sum I_i \times 100\%$$

where I_i is the intensity of the strongest peak in the compound i. Thermal mechanical analysis (TMA) was conducted to analyse the shrinkage behaviour of each specimen at a heating rate of 5 °C min^{-1}. Platinum foils covered both sides of the specimens to avoid contamination from occurring between specimens and the supports. Microstructural evolution of the specimens was studied on a scanning electron microscope (SEM). Dielectric properties were measured in a heating/cooling chamber by a computerized impedance analyser.

3. Results and discussion

3.1. Phase formation process

The thermal variation during the reaction of the raw materials for $Pb(Mg_{0.5}W_{0.5})O_3$, $Pb(Mg_{0.5}W_{0.5})_{0.9}Ti_{0.1}O_3$ and $Pb(Mg_{0.5}W_{0.5})_{0.6}Ti_{0.4}O_3$ was traced by DTA, and those results are illustrated in Fig. 1. At low temperature range, the behaviour of each specimen was similar. A large exothermic reaction occurred at around 300 to 400 °C, and an endothermic peak was formed at 720 °C. The large exothermic reaction was formed due to the combustion of resin mixed with specimens in the ball-milling process. The endothermic peaks at around 720 °C are considered to be caused by the eutectic melting of PbO and the intermediate compound Pb_2WO_5 [14]. No further change was observed in $Pb(Mg_{0.5}W_{0.5})O_3$ on heating above 650 °C; however, an endothermic reaction was found to occur in $Pb(Mg_{0.5}W_{0.5})_{0.9}Ti_{0.1}O_3$ and $Pb(Mg_{0.5}W_{0.5})_{0.6}Ti_{0.4}O_3$ at 890 and 880 °C, respectively. When cooling runs were conducted from 900 °C, exothermic peaks corresponding to the above endothermic peaks were found to occur at 870 and 860 °C for $Pb(Mg_{0.5}W_{0.5})_{0.9}Ti_{0.1}O_3$ and $Pb(Mg_{0.5}W_{0.5})_{0.6}Ti_{0.4}O_3$, respectively. The exothermic peaks during cooling are considered to be caused by the solidification of a liquid phase. Therefore, the corresponding endothermic peaks during heating are due to the formation of a liquid phase. On the other hand, no evidence of liquid phase formation was found in $Pb(Mg_{0.5}W_{0.5})O_3$.

A series of specimens of the raw materials $Pb(Mg_{0.5}W_{0.5})O_3$, $Pb(Mg_{0.5}W_{0.5})_{0.9}Ti_{0.1}O_3$, and $Pb(Mg_{0.5}W_{0.5})_{0.6}Ti_{0.4}O_3$ were heated at a rate of 5 °C min^{-1} and quenched at the desired temperatures in air to study the variation in the resulting products

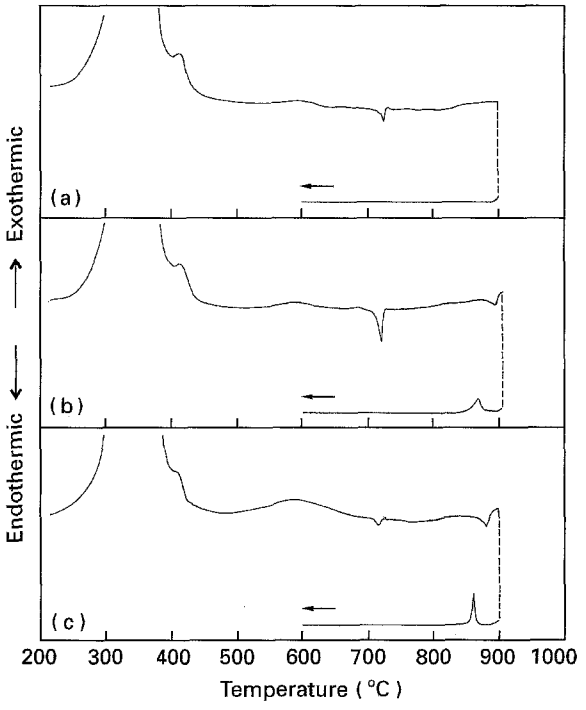

Figure 1 Differential thermal analysis of the raw materials of (a) $Pb(Mg_{0.5}W_{0.5})O_3$, (b) $Pb(Mg_{0.5}W_{0.5})_{0.9}Ti_{0.1}O_3$, and (c) $Pb(Mg_{0.5}W_{0.5})_{0.6}Ti_{0.4}O_3$.

and related reaction sequence. The quenched specimens were analysed by XRD and the formation diagrams are indicated in Figs 2 to 4. In the $Pb(Mg_{0.5}W_{0.5})O_3$ system, the first reaction was between PbO and WO_3, forming the first kind of lead tungstate, $PbWO_4$. $PbWO_4$ then went on to react with PbO, producing the second kind of lead tungstate, Pb_2WO_5, at temperatures from 500 °C. Above 600 °C, the formation of perovskite $Pb(Mg_{0.5}W_{0.5})O_3$ began. The amount of $Pb(Mg_{0.5}W_{0.5})O_3$ increased with temperature, and was associated with the consumption of $PbWO_4$ and Pb_2WO_5. $PbWO_4$ completely disappeared at 720 °C. After Pb_2WO_5 vanished at 850 °C, the formation of $Pb(Mg_{0.5}W_{0.5})O_3$ was accomplished with no other intermediate compounds remaining.

Compared with $Pb(Mg_{0.5}W_{0.5})O_3$, in the $Pb(Mg_{0.5}W_{0.5})_{0.9}Ti_{0.1}O_3$ and $Pb(Mg_{0.5}W_{0.5})_{0.6}Ti_{0.4}O_3$ systems (see Figs 3 and 4), $PbWO_4$ and Pb_2WO_5 were also formed as intermediate compounds in the reaction process; however, the presence of these intermediate compounds maintained at higher temperatures. Consequently, these lead tungstates postponed the complete formation of the perovskite phases of $Pb(Mg_{0.5}W_{0.5})_{0.9}Ti_{0.1}O_3$ and

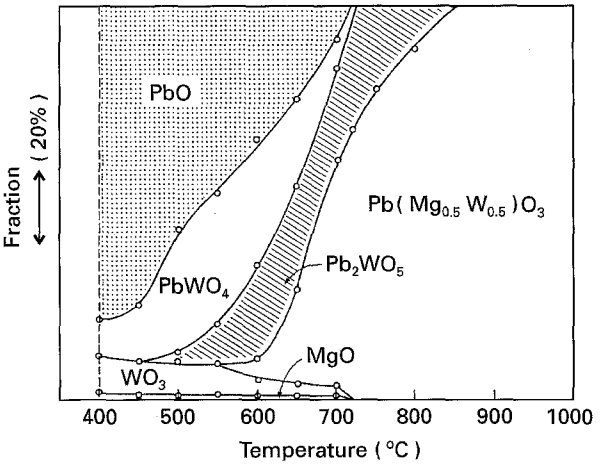

Figure 2 Formation diagram of $Pb(Mg_{0.5}W_{0.5})O_3$ in solid-state reaction.

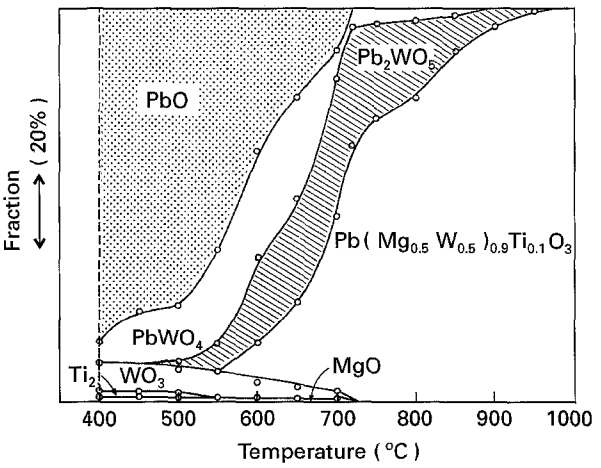

Figure 3 Formation diagram of $Pb(Mg_{0.5}W_{0.5})_{0.9}Ti_{0.1}O_3$ in solid-state reaction.

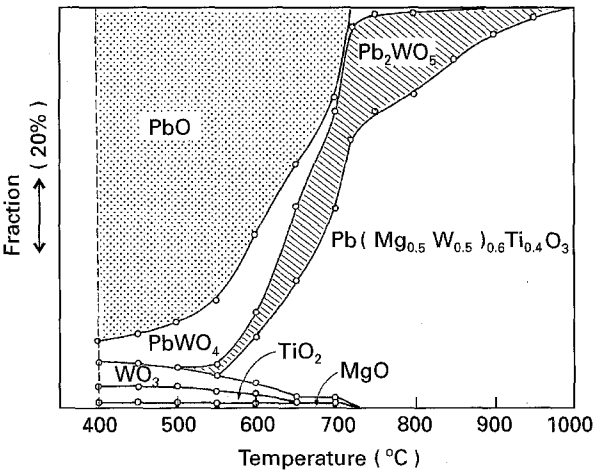

Figure 4 Formation diagram of $Pb(Mg_{0.5}W_{0.5})_{0.6}Ti_{0.4}O_3$ in solid-state reaction.

$Pb(Mg_{0.5}W_{0.5})_{0.6}Ti_{0.4}O_3$. Heating temperatures were raised to 900 and 1000 °C to result in the complete elimination of $PbWO_4$ and Pb_2WO_5. As a result, the temperature for the complete reaction of $Pb(Mg_{0.5}W_{0.5})_{0.9}Ti_{0.1}O_3$ and $Pb(Mg_{0.5}W_{0.5})_{0.6}Ti_{0.4}O_3$ had to increase up to 1000 °C. It was noted that in all of the above systems, no pyrochlore phase was formed in the reaction process. This is different from the formation processes in general relaxor systems [15, 16]. $Pb(Mg_{0.5}W_{0.5})O_3$ exhibited an orthorhombic structure. Both $Pb(Mg_{0.5}W_{0.5})_{0.9}Ti_{0.1}O_3$ and $Pb(Mg_{0.5}W_{0.5})_{0.6}Ti_{0.4}O_3$ exhibited cubic structure. These results are identical to those found in previous literature [17]. The difference in crystalline structure revealed that the ambient temperature of XRD measurement was lower than the Curie temperature of $Pb(Mg_{0.5}W_{0.5})O_3$, but higher than those of $Pb(Mg_{0.5}W_{0.5})_{0.9}Ti_{0.1}O_3$ and $Pb(Mg_{0.5}W_{0.5})_{0.6}Ti_{0.4}O_3$. These results coincide with the dielectric properties that are shown in section 3.4. Strong superlattice diffraction lines were observed for $Pb(Mg_{0.5}W_{0.5})O_3$; however, no such lines were found for $Pb(Mg_{0.5}W_{0.5})_{0.9}Ti_{0.1}O_3$ and $Pb(Mg_{0.5}W_{0.5})_{0.6}Ti_{0.4}O_3$. This implies that the addition of $PbTiO_3$ in $Pb(Mg_{0.5}W_{0.5})O_3$ resulted in a random arrangement of Mg^{2+}, W^{6+}, and Ti^{4+} cations located in oxygen octahedrons. The reason for the disordered arrangement of cations was considered to be that Ti^{4+} has a similar ionic radius to those of Mg^{2+} and W^{6+} (Ti^{4+}: 0.068 nm, Mg^{2+}: 0.065 nm, and W^{6+}: 0.068 nm) and the presence of Ti^{4+} decreased the charge difference of the cations in the B sites.

From the formation diagrams, the reaction sequences of $Pb(Mg_{0.5}W_{0.5})O_3$ can be deduced to be

$$PbO + WO_3 \xrightarrow{400\text{–}720\,^\circ C} PbWO_4 \quad (1)$$

$$PbWO_4 + WO_3 \xrightarrow{500\text{–}850\,^\circ C} Pb_2WO_5 \quad (2)$$

$$Pb_2WO_5 + MgO \xrightarrow{600\text{–}850\,^\circ C} 2Pb(Mg_{0.5}W_{0.5})O_3 \quad (3)$$

In the $Pb(Mg_{0.5}W_{0.5})_{0.9}Ti_{0.1}O_3$ and $Pb(Mg_{0.5}W_{0.5})_{0.6}Ti_{0.4}O_3$ systems, the reaction sequences are summarized as follows:

$$PbO + WO_3 \xrightarrow{400\text{–}900\,^\circ C} PbWO_4 \quad (4)$$

$$PbWO_4 + WO_3 \xrightarrow{600\text{–}1000\,^\circ C} Pb_2WO_5 \quad (5)$$

$$(1-x)Pb_2WO_5 + (1-x)MgO + 2xTiO_2 + 2xPbO \xrightarrow{550\text{–}1000\,^\circ C} 2Pb(Mg_{0.5}W_{0.5})_{1-x}Ti_xO_3 (x = 0.1 \text{ and } 0.4) \quad (6)$$

In the $PbTiO_3$-doped $Pb(Mg_{0.5}W_{0.5})O_3$ systems, reaction (6) is more complicated than reaction (3) for $Pb(Mg_{0.5}W_{0.5})O_3$. The interdiffusion of each species would become insufficient when the number of the species involved in the reaction increases. Consequently, the insufficient interdiffusion would result in the retardation of the reaction.

3.2. Liquid phase formation

Liquid phases were evidenced by the DTA results (Fig. 1) in $Pb(Mg_{0.5}W_{0.5})_{0.9}Ti_{0.1}O_3$ and $Pb(Mg_{0.5}W_{0.5})_{0.6}Ti_{0.4}O_3$ systems. In the aforementioned two materials, Pb_2WO_5 was present at elevated temperatures in the final reaction process (see Figs 3 and 4). Although the direct melting of Pb_2WO_5 (m.p. = 935 °C) could not account for the liquid phase formation [14], other residual species, e.g. TiO_2 or MgO, present in samples may reduce the melting temperature of Pb_2WO_5 to form a liquid phase at around 880–890 °C. Similar phenomena could also be found in the $Pb(Fe_{0.67}W_{0.33})O_3$ system [18]. Fe_2O_3 reduced the melting temperature of Pb_2WO_5, thereby resulting in the formation of a liquid phase at 860 °C. On the other hand, in $Pb(Mg_{0.5}W_{0.5})O_3$, all of the Pb_2WO_5 was reacted to form $Pb(Mg_{0.5}W_{0.5})O_3$ below 850 °C, that is, no Pb_2WO_5 was present in the specimens at high temperatures. This would account for why no liquid phase was formed in the $Pb(Mg_{0.5}W_{0.5})O_3$ system.

Fig. 5 indicates the shrinkage behaviour of each mixed material as examined by TMA. A small degree of expansion was observed in all the specimens at low temperature range. This expansion was associated with the formation of $PbWO_4$ and Pb_2WO_5. After being heated to 700 °C, all of the specimens began to shrink. This is because the densities of $Pb(Mg_{0.5}W_{0.5})O_3$, $Pb(Mg_{0.5}W_{0.5})_{0.9}Ti_{0.1}O_3$, and $Pb(Mg_{0.5}W_{0.5})_{0.6}Ti_{0.4}O_3$ ($d = 9.39$, 9.248, 8.874 $g\,cm^{-3}$, respectively [17] are larger than that of the major reactant Pb_2WO_5 ($d = 8.109\ g\,cm^{-3}$). The $Pb(Mg_{0.5}W_{0.5})O_3$ specimen shrank smoothly up to 1000 °C; on the other hand, the shrinkage rate increased from about 880 °C in the $PbTiO_3$-doped systems (Fig. 5b and c). The temperature for the rapid specimen shrinkage in TMA was notably close to the formation temperature of the liquid phase in DTA (Fig. 1). This fact would imply that the liquid phase accelerated the shrinkage rate of the specimens through the mechanism of liquid phase sintering.

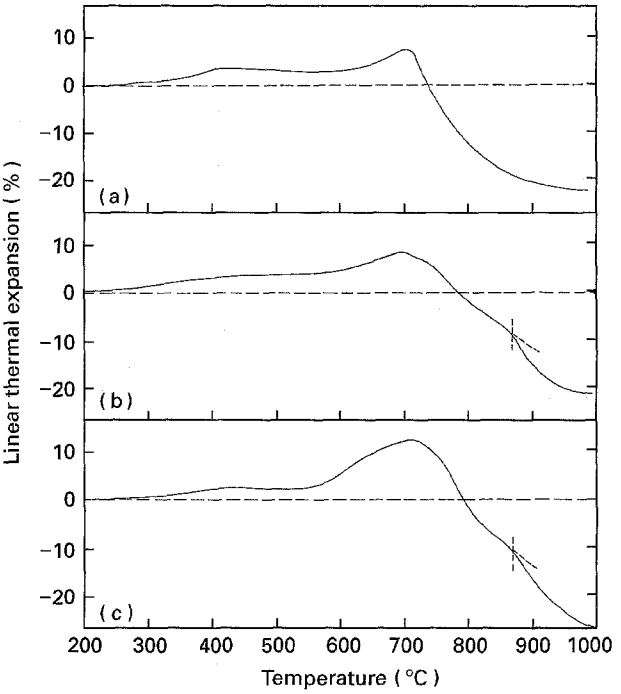

Figure 5 Thermal–mechanical analysis of the raw materials of (a) $Pb(Mg_{0.5}W_{0.5})O_3$, (b) $Pb(Mg_{0.5}W_{0.5})_{0.9}Ti_{0.1}O_3$, and (c) $Pb(Mg_{0.5}W_{0.5})_{0.6}Ti_{0.4}O_3$.

3.3. Microstructural evolution

The microstructure of different samples quenched at 800 and 1000 °C was observed by SEM. The micrographs are shown in Figs 6 and 7. At 800 °C, the pure perovskite phase of $Pb(Mg_{0.5}W_{0.5})O_3$ was completely formed and the particle size was about 0.6–0.7 μm. On the other hand, in $Pb(Mg_{0.5}W_{0.5})_{0.9}Ti_{0.1}O_3$ and $Pb(Mg_{0.5}W_{0.5})_{0.6}Ti_{0.4}O_3$ the formation of perovskite phase was not complete, and the secondary phase Pb_2WO_5 (the dark region with particle sizes about 5 μm at the right corner of Fig. 6b and c) still remained in the specimens. This result was consistent with the XRD results (Figs 3 and 4). When the specimens were heated to 1000 °C, the grain size of $Pb(Mg_{0.5}W_{0.5})O_3$ increased to about 5 to 7 μm (Fig. 7a). At 1000 °C in the $Pb(Mg_{0.5}W_{0.5})_{0.9}Ti_{0.1}O_3$ and $Pb(Mg_{0.5}W_{0.5})_{0.6}Ti_{0.4}O_3$ systems (Fig. 7b and c), Pb_2WO_5 grains completely disappeared, and only perovskite-phase grains remained. It is noted that $Pb(Mg_{0.5}W_{0.5})_{0.9}Ti_{0.1}O_3$ and $Pb(Mg_{0.5}W_{0.5})_{0.6}Ti_{0.4}O_3$ had a more densified microstructure than that of $Pb(Mg_{0.5}W_{0.5})O_3$. However, their microstructure was not homogeneous. The grain size of $Pb(Mg_{0.5}W_{0.5})_{0.9}Ti_{0.1}O_3$ and $Pb(Mg_{0.5}W_{0.5})_{0.6}Ti_{0.4}O_3$ exhibited a bimodal distribution with small grains of about 1 to 1.2 μm, and large ones of about 10 μm. This bimodal distribution of grain size was probably caused by the presence of grains that underwent abnormal grain-growth from the liquid phase which existed at the high temperatures. The number of grains that experienced abnormal grain growth in $Pb(Mg_{0.5}W_{0.5})_{0.6}Ti_{0.4}O_3$ was larger than those in $Pb(Mg_{0.5}W_{0.5})_{0.9}Ti_{0.1}O_3$,

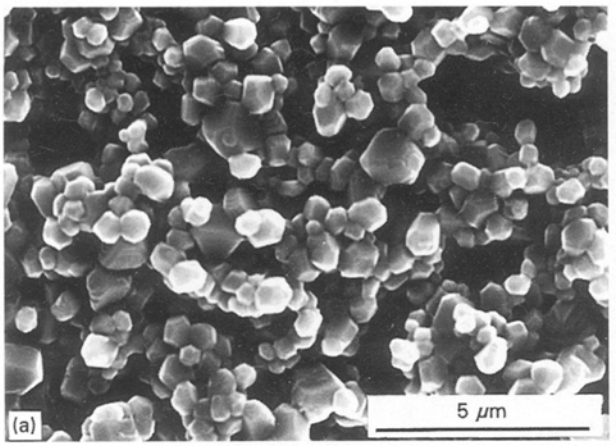

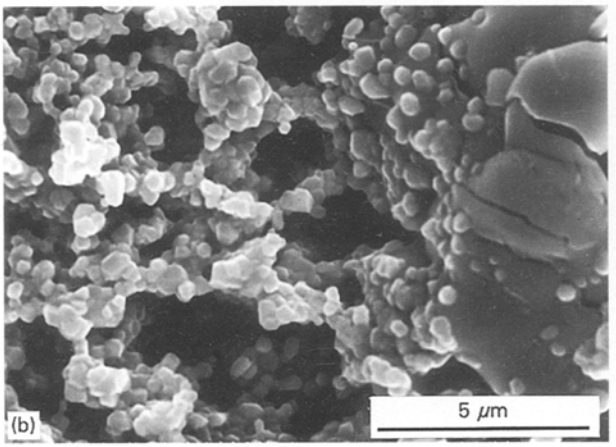

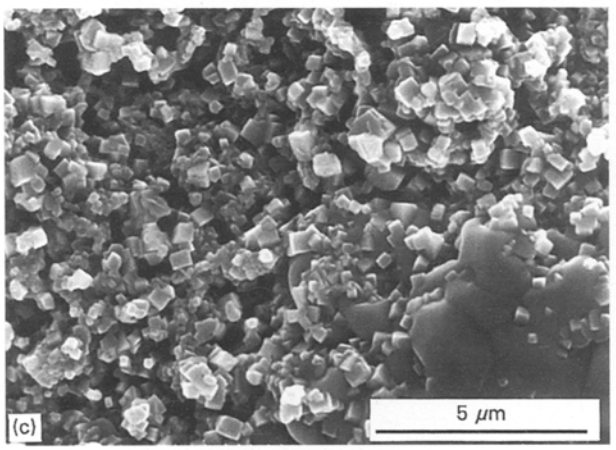

Figure 6 Scanning electron micrographs of (a) $Pb(Mg_{0.5}W_{0.5})O_3$, (b) $Pb(Mg_{0.5}W_{0.5})_{0.9}Ti_{0.1}O_3$, and (c) $Pb(Mg_{0.5}W_{0.5})_{0.6}Ti_{0.4}O_3$ quenched at 800 °C.

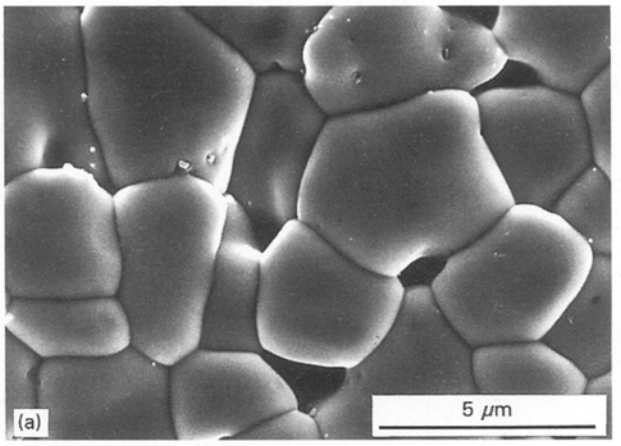

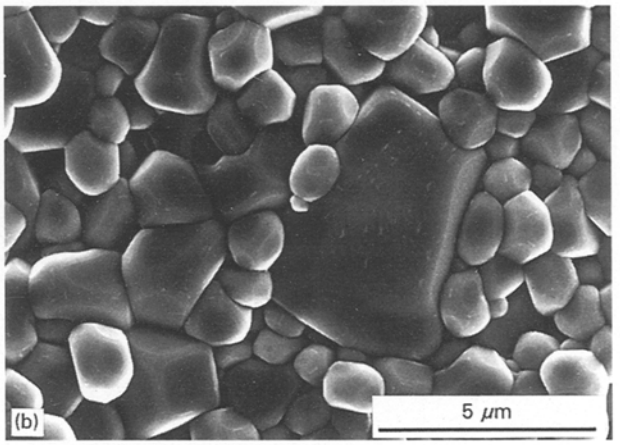

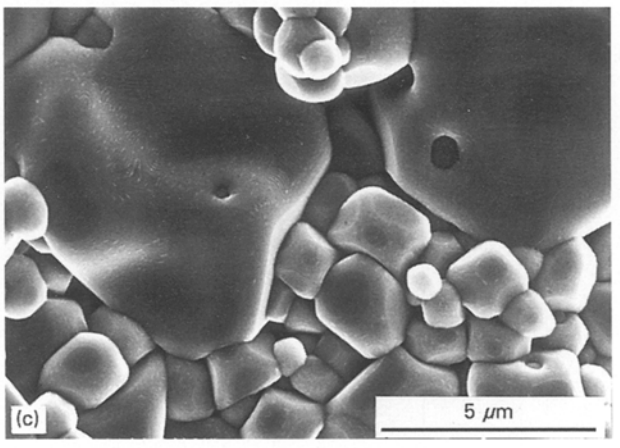

Figure 7 Scanning electron micrographs of (a) $Pb(Mg_{0.5}W_{0.5})O_3$, (b) $Pb(Mg_{0.5}W_{0.5})_{0.9}Ti_{0.1}O_3$, and (c) $Pb(Mg_{0.5}W_{0.5})_{0.6}Ti_{0.4}O_3$ quenched at 1000 °C.

implying that the amount of liquid phase in $Pb(Mg_{0.5}W_{0.5})_{0.6}Ti_{0.4}O_3$ seems to have been more than that in $Pb(Mg_{0.5}W_{0.5})_{0.9}Ti_{0.1}O_3$. The DTA results (see Fig. 1b and c) support the above discussion since the exothermic peak in the cooling run for $Pb(Mg_{0.5}W_{0.5})_{0.6}Ti_{0.4}O_3$ was larger than that for $Pb(Mg_{0.5}W_{0.5})_{0.9}Ti_{0.1}O_3$.

3.4. Dielectric properties

The temperature and frequency dependencies of dielectric permittivity for each sintered sample are shown in Figs 8 to 10. A sharp permittivity maximum occurred in $Pb(Mg_{0.5}W_{0.5})O_3$ at around 40 °C with a value around 200. When the measurement frequency was changed, almost all of the data overlapped (see Fig. 8). The overlapping indicates that no dielectric dispersion occurred. In contrast, when $Pb(Mg_{0.5}W_{0.5})O_3$ was doped with $PbTiO_3$, these doped samples exhibited strong dielectric dispersion with frequency, i.e. a diffuse phase transition. As the measurement frequency was increased from 1 kHz to 1 MHz in $Pb(Mg_{0.5}W_{0.5})_{0.9}Ti_{0.1}O_3$, the maximum dielectric temperature (T_m) increased from -104 to -92 °C, and the maximum dielectric constant (k_m) decreased from 800 to 740 (see Fig. 9). A similar frequency dependence could also be observed in $Pb(Mg_{0.5}W_{0.5})_{0.6}Ti_{0.4}O_3$. When the frequency was raised from 1 kHz to 1 MHz, T_m increased from

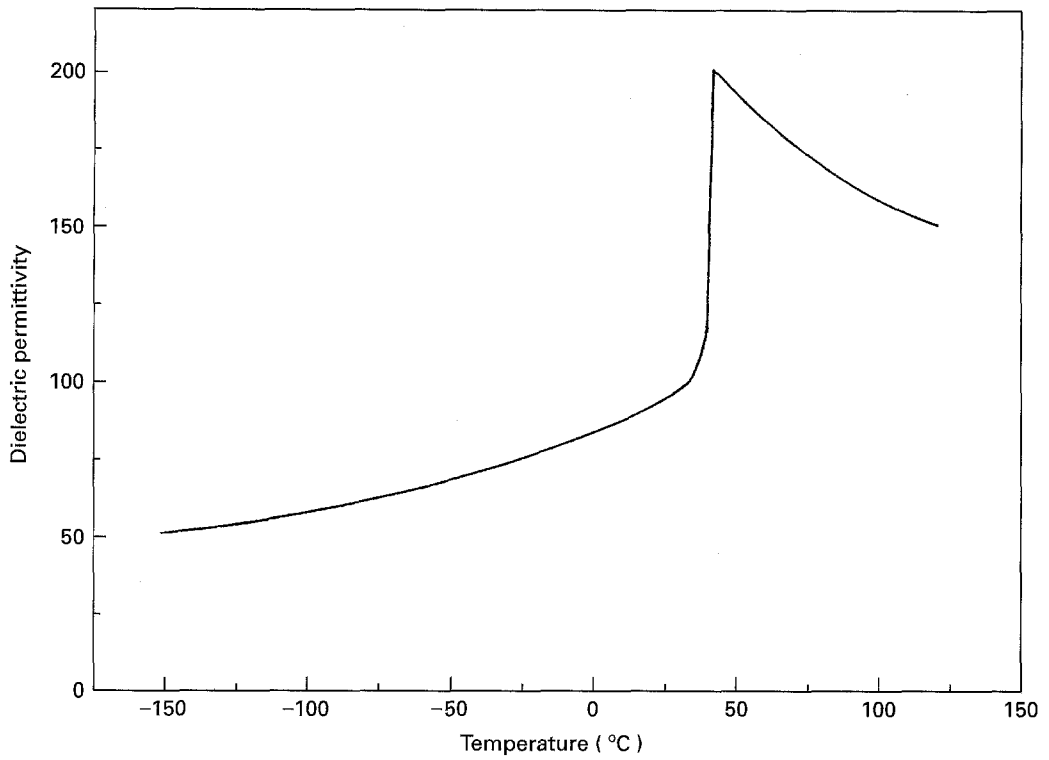

Figure 8 Dielectric permittivity of $Pb(Mg_{0.5}W_{0.5})O_3$. The data at 1, 10, 100 kHz, and 1 MHz all overlap.

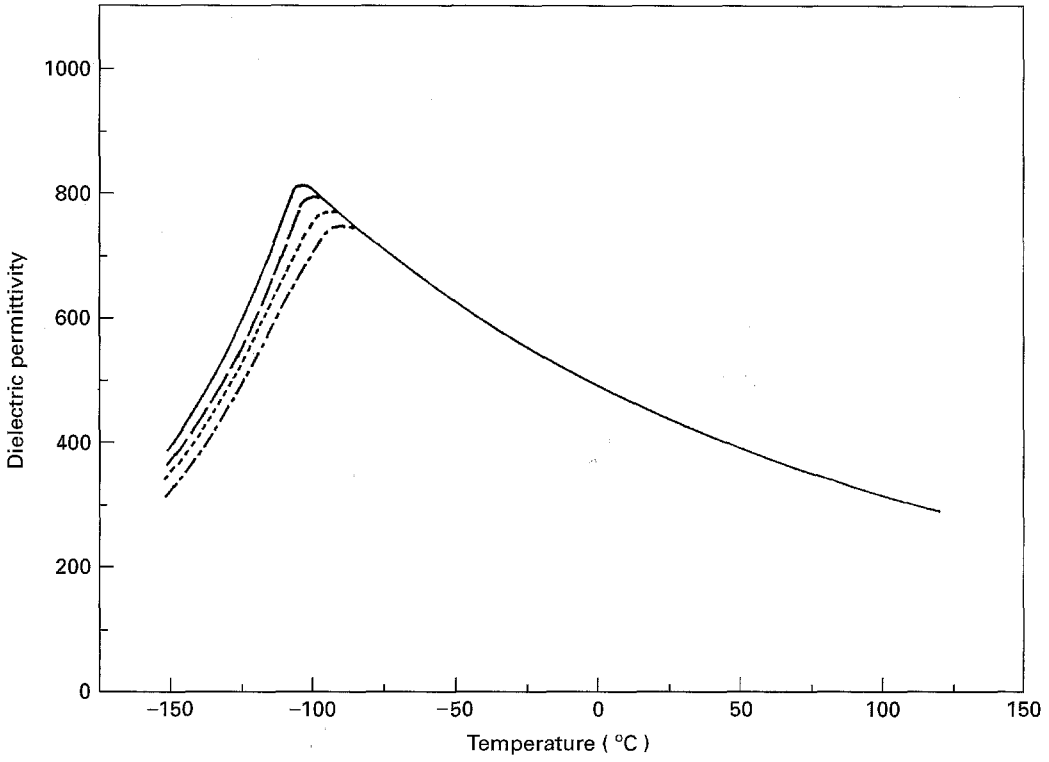

Figure 9 Dielectric permittivity of $Pb(Mg_{0.5}W_{0.5})_{0.9}Ti_{0.1}O_3$ at 1 (—), 10 (– – –), 100 kHz (- - - -), and 1 MHz; (— — — —).

0 to 25 °C and k_m decreased from 6000 to 5500 (see Fig. 10). Compared with $Pb(Mg_{0.5}W_{0.5})_{0.9}Ti_{0.1}O_3$, $Pb(Mg_{0.5}W_{0.5})_{0.6}Ti_{0.4}O_3$ has a maximum dielectric constant one order higher, and a much broader dielectric maximum. According to the results of Smolenskii *et al.* [5], below the transition temperatures, $Pb(Mg_{0.5}W_{0.5})O_3$ shows antiferroelectric properties; meanwhile, $Pb(Mg_{0.5}W_{0.5})_{0.9}Ti_{0.1}O_3$ and $Pb(Mg_{0.5}W_{0.5})_{0.6}Ti_{0.4}O_3$ show ferroelectric properties. Thus, from a comparison with the work of Smolenskii *et al.* [5] to the results obtained in this study, the sharp phase transformation of $Pb(Mg_{0.5}W_{0.5})O_3$ is a typical antiferroelectric/paraelectric type; on the other hand, these two $PbTiO_3$-doped samples exhibit a broad relaxor ferroelectric type of phase transformation. The fact that the broadness of the dielectric maximum increased with $PbTiO_3$ amount implies that adding $PbTiO_3$ to

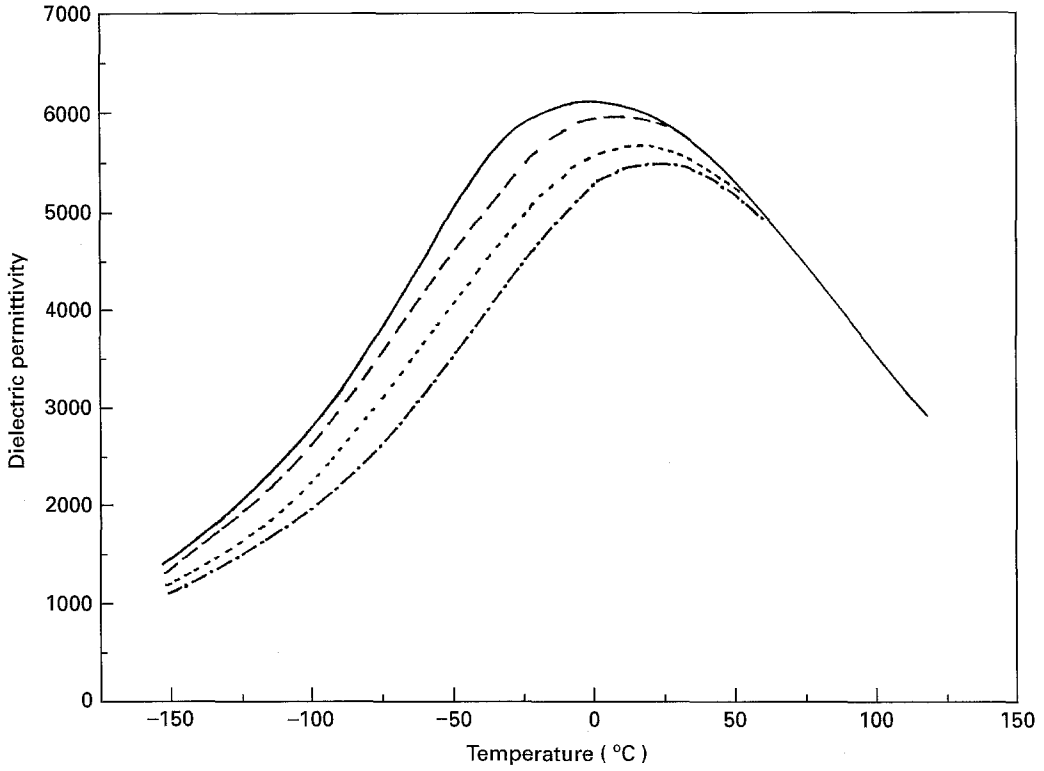

Figure 10 Dielectric permittivity of $Pb(Mg_{0.5}W_{0.5})_{0.6}Ti_{0.4}O_3$ at 1 (—), 10 (– – –), 100 kHz (- - - -), and 1 MHz; (— — — —).

$Pb(Mg_{0.5}W_{0.5})O_3$ alters the arrangement of B-site cations located in oxygen octahedrons from an ordered to a disordered state, thereby inducing the diffuse phase transition behaviour.

4. Conclusion

The perovskite phase formation and microstructural evolution of the lead magnesium tungstate–lead titanate ceramics have been investigated in this study. Only $PbWO_4$ and Pb_2WO_5 are formed as the intermediate phases in the reaction. As $Pb(Mg_{0.5}W_{0.5})O_3$ is doped with $PbTiO_3$, the perovskite phase formation in $Pb(Mg_{0.5}W_{0.5})_{0.9}Ti_{0.1}O_3$ and $Pb(Mg_{0.5}W_{0.5})_{0.6}Ti_{0.4}O_3$ is retarded and forced to reach completion at a higher temperature than occurs in $Pb(Mg_{0.5}W_{0.5})O_3$. A liquid phase is formed in $Pb(Mg_{0.5}W_{0.5})_{0.9}Ti_{0.1}O_3$ and $Pb(Mg_{0.5}W_{0.5})_{0.6}Ti_{0.4}O_3$, which is ascribed to the reaction with residual Pb_2WO_5. This liquid phase accelerates the shrinkage of specimens, but also results in an inhomogeneous microstructure. $Pb(Mg_{0.5}W_{0.5})O_3$ exhibits a sharp phase transformation from an antiferroelectric to a paraelectric state at around 40 °C; in addition, its dielectric permittivity does not have any frequency dependence. However, $Pb(Mg_{0.5}W_{0.5})_{0.9}Ti_{0.1}O_3$ and $Pb(Mg_{0.5}W_{0.5})_{0.6}Ti_{0.4}O_3$ exhibit a broad phase transformation; moreover, their dielectric properties strongly depend on frequency. The various phase-transformation behaviours indicate that the addition of $PbTiO_3$ to $Pb(Mg_{0.5}W_{0.5})O_3$ alters the arrangement of B-site cations from an orderly to a disorderly state, thereby inducing relaxor ferroelectric characteristics.

References

1. W. R. BUESSEM and T. I. PROKOPOWICZ, *Ferroelectrics* **10** (1976) 225.
2. Y. SAKABE, *Amer. Ceram. Soc. Bull.* **66** (1987) 1338.
3. M. YONEZAWA, M. K. UTSUMI and S. SAITO, in "High Tech Ceramics" edited by P. Vincenzini (Elsevier Science Publishers B.V., Amsterdam, 1987) p. 1493.
4. G. A. SMOLENSKII, A. I. AGRANOVSKAYA and V. A. ISUPOV, *Sov. Phys. Tech. Phys.* **1** (1959) 1981.
5. G. A. SMOLENSKII, N. N. KRAINIK and A. I. AGRANOVSKAYA, *Sov. Phys. Solid State* **3** (1961) 714.
6. S. NOMURA, S. J. JANG, L. E. CROSS and R. E. NEWNHAM, *J. Amer. Ceram. Soc.* **62** (1979) 485.
7. S. NOMURA, J. KUWATA, K. UCHINO, S. J. JANG, L. E. CROSS and R. E. NEWNHAM, *Phys. State Solid* **57** (1980) 317.
8. Ya. S. BOGDANOV, A. Ya. DANTSIGER, O. N. RAZUMOVSKAYA and E. G. FESENKO, *Inorg. Mater.* **17** (1981) 12.
9. M. H. LEE and W. K. CHOO, *J. Appl. Phys.* **52** (1981) 5767.
10. T. KOBAYASHI, S. SUGIYAMA and K. UCHINO, *Ferroelectrics Lett.* **7** (1987) 75.
11. R. J. BOUCHARD, L. H. BRIXNER and M. J. POPOWICH, US Patent 4228482 October (1980).
12. M. YONEZAWA, *Ferroelectrics* **68** (1986) 181.
13. S. TAKAHASHI, A OCHI, K. UTSUMI and M. SHIRAKATA, *Jpn. J. Appl. Phys.* **28** (1989) 35.
14. L. L. Y. CHANG, *J. Amer. Ceram. Soc.* **54** (1971) 357.
15. M. LEJUENE and J. P. BIOLOT, *Ceram. Int.* **8** (1982) 99.
16. C. H. LU, K. SHINOZAKI, N. MIZUTANI, and M. KATO, *J. Jpn. Ceram. Soc.* **97** (1989) 119.
17. A. I. ZASLAVSKII and M. F. BRYZHINA, *Sov. Phys. Cryst.* **7** (1963) 577.
18. C. H. LU, *J. Amer. Ceram. Soc.* **73** (1994) 2529.

Received 23 August 1994
and accepted 22 June 1995